



Ultra-sensitive fluid fill height sensing based on spoof surface plasmon polaritons

Li Chen, Henghui Yin, Lin Chen & Yiming Zhu

To cite this article: Li Chen, Henghui Yin, Lin Chen & Yiming Zhu (2018) Ultra-sensitive fluid fill height sensing based on spoof surface plasmon polaritons, Journal of Electromagnetic Waves and Applications, 32:4, 471-482, DOI: [10.1080/09205071.2017.1395367](https://doi.org/10.1080/09205071.2017.1395367)

To link to this article: <https://doi.org/10.1080/09205071.2017.1395367>



Published online: 28 Oct 2017.



Submit your article to this journal [↗](#)



Article views: 27



View related articles [↗](#)



View Crossmark data [↗](#)



Ultra-sensitive fluid fill height sensing based on spoof surface plasmon polaritons

Li Chen^a, Henghui Yin^a, Lin Chen^{a,b}  and Yiming Zhu^{a,b}

^aShanghai Key Lab of Modern Optical System, University of Shanghai for Science and Technology, Shanghai, China; ^bCooperative Innovation Center of Terahertz Science, University of Electronic Science and Technology, Chengdu, China

ABSTRACT

We analyzed fluid fill height sensing supported by terahertz spoof surface plasmon polaritons (SPPs). The existence of spoof SPPs was proved experimentally and was discussed from perspective of dispersion and field distribution. For the application, we designed a fluid fill height sensor based on spoof SPPs, which is much more sensitive than previous work based on parallel plate waveguide (PPWG). For example, resonant shift of spoof SPPs is almost four times larger than the shift of PPWG at the height of 250 μm . This fluid fill height sensor calibrated the fluid volume in grooves, which contributes to improving the accuracy of high refractive index sensing. The experiment is in good agreement with simulation. Such proposed fluid height sensor has another advantage of being suitable for the fluid with refractive index higher than prism, which further benefits spoof SPPs refractive index sensing, such as blood detection in future.

ARTICLE HISTORY

Received 5 June 2017
Accepted 12 October 2017

KEYWORDS

Spoof surface plasmons; terahertz; fluid fill height sensing; refractive index

1. Introduction

Surface plasmon polaritons (SPPs) are created by the coupling of light to collective oscillation of electrons on the conducting material, which propagate along the conductive/dielectric interface non-radiatively [1,2]. Owing to the ability to spatially confine the electromagnetic wave within sub-wavelength and tremendously enhance the electromagnetic field intensity within a confined region [3], SPPs are often utilized for sensing [4,5]. However, metal can be regarded as a perfect electric conductor (PEC) in terahertz (THz) range, which results in the weakly bounded SPPs to the smooth metal/dielectric interface. Fortunately, this problem can be circumvented by the concept of THz structured surface [6–13]. Note that the plasmon polaritons mentioned in our work are excited in structured metal surface at low frequency (THz), which are called spoof SPPs [6]. Real SPPs can be excited efficiently on metal–dielectric surface at visible frequencies.

We note that, spoof SPPs sensing has been well discussed in THz range [14–18]. Ng et al. [14] investigated the spectral shift of spoof SPPs from 1D periodic grooves as a function of refractive index change via terahertz time-domain spectroscopy (THz-TDS). Yao et al. [15] proposed the high-mode spoof SPPs of periodic metal grooves for ultra-sensitive terahertz

refractive index sensing. Quite recently, Zhang et al. [16] analyzed the angular dependence of the resonant angle to the refractive index change. In general, the majority of applications using spoof SPPs are refractive index sensing, the fluid fill height sensing is less explored. Astley et al. [19] researched resonant shift from singly grooved parallel-plate waveguide (PPWG) as a function of fluid fill height in a rectangular groove, however the sensitivity is not very high. In this paper, we mainly investigated the application of fluid fill height sensing supported by spoof SPPs, which contributes to improving the accuracy of high refractive index sensing. We first presented the sensing platform and proved the existence of spoof SPPs in 1D periodic grooves. Then, we analyzed the reason for generation of spoof SPPs from the perspective of dispersion and field distribution. After this, the sensing platform applied to detect fluid fill height in rectangular grooves was discussed theoretically and experimentally in detail. The spoof SPPs have a much larger interaction length (several grooves) than the rather limited interaction length (single groove) of PPWG, so the fluid fill height sensing based on spoof SPPs is much more sensitive to that based on PPWG [19] with only single groove. The PPWG cavity mode was discussed in detail in previous work [20–22]. Such fluid fill height sensing can be used to calibrate the fluid volume in the groove, which contributes to improving the accuracy of high refractive index sensing. The fluid height sensor we proposed here refers to the detection of fluid refractive index higher than the refractive index of prism.

2. The experiment of spoof SPPs

Our sensing configuration is the conventional Otto prism-coupling model [23], as shown in Figure 1. It consists of a coupling prism and a metal film etched by a 1D groove structure with period $p = 300 \mu\text{m}$, height $h = 180 \mu\text{m}$ and width $w = 180 \mu\text{m}$. The distance gap

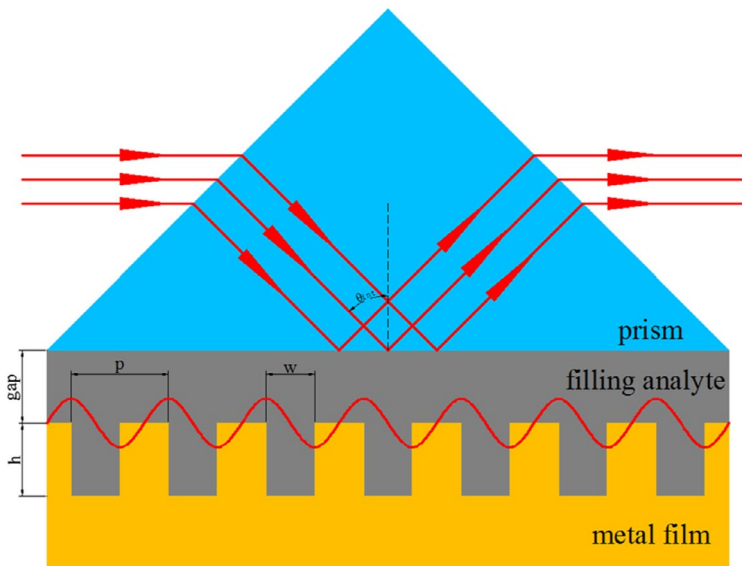


Figure 1. The Otto sensing configuration. The metal film is etched with rectangular groove with period p , height h and width w . The gap is distance between prism and metal film. The θ_{int} is internal incident angle at bottom of prism.

between prism and film is filled with fluid with refractive index n_d . The prism composed of Teflon with high refractive index $n_p = 1.446$ is used for phase-matching, in order to excite spoof SPPs on the metal film. The $\theta_{\text{int}} = 74.28^\circ$ is internal incident angle at bottom of prism. The total internal reflection occurs when the θ_{int} is larger than the critical angle. The permittivity of metal is described by Drude model. Here, the metal is supposed to be Cu with plasma frequency $w_p = 1.12 \times 10^{16}$ Hz and scattering frequency $\gamma = 8.67 \times 10^{13}$ Hz [24,25].

The experiment was carried out through THz-TDS [26–28] in a dry air purged chamber with relative humidity less than 5%. A collimated THz beam from the THz-TDS emitter injects into the prism and refracts at the bottom with an incident angle θ_{int} . The evanescent wave generated at the bottom of the prism interacts with the fluid inside the gap and grooves and then excites the propagating attenuated spoof SPPs wave on the surface of the groove structure when the momentum matching condition is satisfied. The corresponding resonance frequency component will vanish in the collimated THz beam detected by the THz-TDS detector. The frequency spectrum can be obtained from the time-domain signal via a Fourier Transform. Assuming that the detected signal reflected off the prism with spoof SPPs is E_{sam} and the signal in the absence of spoof SPPs is E_{ref} , then the experimental THz reflectivity can be defined as $R = |E_{\text{sam}}/E_{\text{ref}}|^2$. As can be seen from Figure 2, there is a dip at 0.265 THz in reflectivity spectrum, which proves the existence of spoof SPPs effectively.

3. The discussion of spoof SPPs

The wave-vector of the incident light in the prism can be expressed as $k_p = n_p w/c = k_{\perp}^2 + k_{\parallel}^2$, where k_{\perp} and k_{\parallel} are parallel and perpendicular components of the wave-vector, respectively. The spoof SPPs phenomenon will show up when the following condition is satisfied:

$$k_{\text{spoofSPPs}} = k_{\parallel} = k_p \sin \theta_{\text{int}} \quad (1)$$

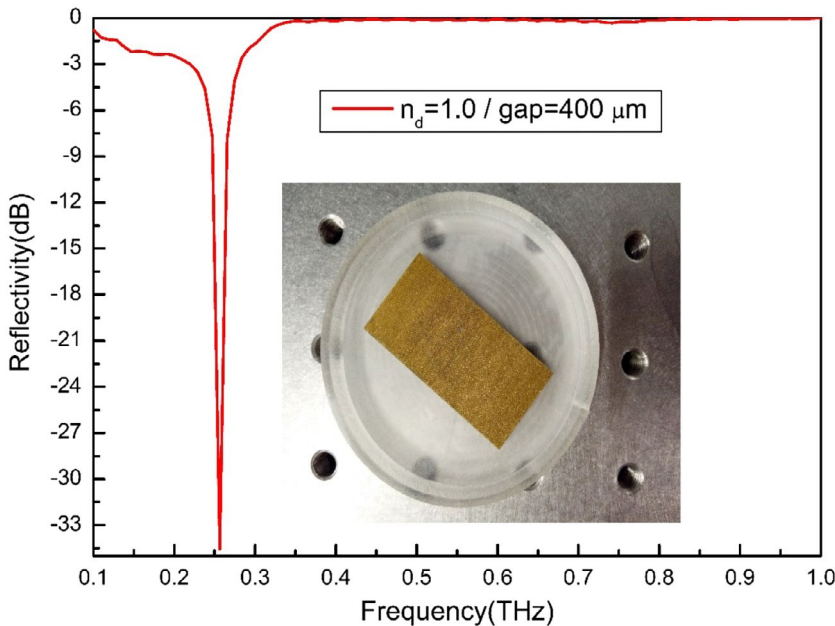


Figure 2. The reflectivity spectrum of sensing system obtained from THz-TDS with gap = 400 μm .

For the spoof SPPs sensor with wavelength modulation, the incident light will couple into spoof SPPs when the above-mentioned condition is satisfied and a sharp dip will appear in the reflection spectrum. The dispersion relation of rectangular groove is demonstrated in Figure 3. This dispersion curve of spoof SPPs supported by a 1D array of grooves is analyzed using the commercial software CST Microwave Studio in which the unit cell is located in an outer air box. For the air box, the boundaries in the x direction should be set as master and slave boundaries (i.e. the periodic boundary), and the other boundaries in the y and z directions are set as PEC. The air line (blue) and the prism line (green) represent the dispersion relation of incident light in air and parallel wave-vector k_{\parallel} in prism, respectively. The spoof SPPs dispersion curve (black) is close to the air line at low frequency, but deviates from it when approaching to the edge of first Brillouin zone. The prism line will intersect with the spoof SPPs dispersion curve when $k_{\text{spoofSPPs}} = k_p \sin \theta_{\text{int}}$. The frequency at the intersection (black dot A) is just the resonance frequency $f_{\text{sp}} = 0.259$ THz.

In order to describe the spoof SPPs in our sensing system, 2D simulation was carried out to obtain the reflectivity spectrum and field distribution in Figure 4 using COMSOL MULTIPHYSICS software. The model is a periodic structure with a single groove as the unit cell, shown as right inset (b) in Figure 4. The Floquet periodic boundary conditions were applied along the direction of periodicity to imitate the periodic structure. The upper boundary was set the excitation source to inject the P-polarized THz radiation at the incident angle of 74.28° . The refractive index n_p of coupling prism is 1.446 and the domain between prism and metal is set air. A sharp dip appears at the frequency of 0.26 THz where the reflectivity is nearly zero, which demonstrates that most of the incident energy has been coupled into the spoof SPPs. The resonance frequency deviates from the frequency at intersection A.

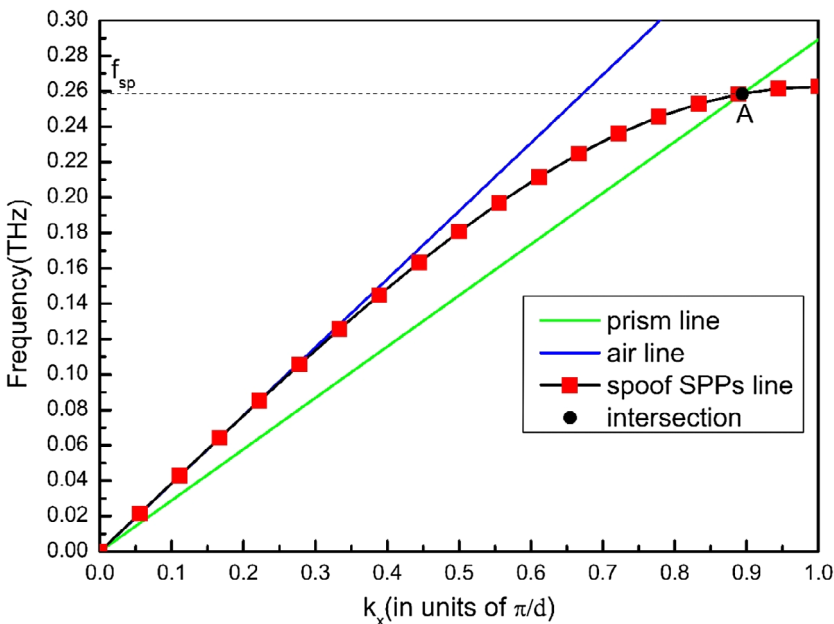


Figure 3. The dispersion relation of spoof SPPs. The air line and prism line are dispersion relation of incident light in air and parallel wave-vector of light in prism, respectively. The frequency at the intersection (A) is just the resonance frequency.

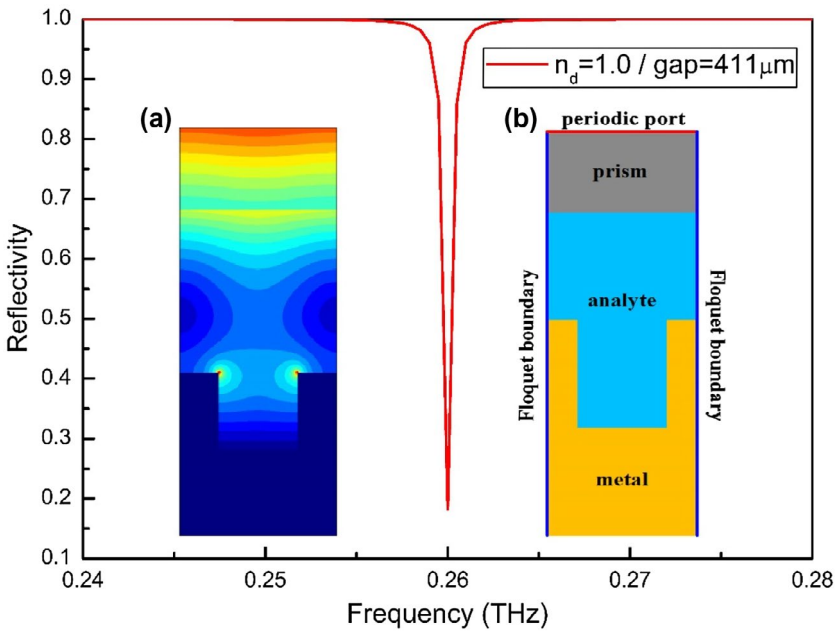


Figure 4. The reflectivity as a function of frequency calculated at the incident angle of 74.28° , with $n_d = 1.0$ and gap = $411 \mu\text{m}$. Left inset (a) is field distribution at 0.26 THz. Right inset (b) is the periodic structure of model.

These deviations occur because the propagating surface plasmon is not theoretical surface wave when gap is small; as a result, a considerable part of the energy will reradiate back into the prism. The reradiation will affect spoof SPPs dispersion relation. In addition, the energy damping [23] and destructive interference effect [29] also affect the shift of resonance. The left inset (a) in Figure 4 is the simulated field distribution at 0.26 THz. It is clear that the fields are tightly confined to the spoof SPPs at resonance frequency, and removed from prism-coupling gap.

4. The analysis of fluid fill height and high refractive index sensing

After realizing the effective excitation of spoof SPPs in metal grating, this platform can evaluate fluid fill height in the groove, which contributes to improving the accuracy of high refractive index sensing. A unit cell of height sensor is demonstrated in Figure 5(a), which has four layers. The fluid used here is tetradecane with a refractive index $n = 1.4224$ at room temperature, which exhibits very low absorption and almost no dispersion in THz range [30]. The fluid is put into rectangular groove and the height of fluid lower than or equal to depth of groove.

From the beginning of an empty groove and calculating resonance frequency for these grooves as they are filled with fluid gradually, then the resonant shift verse height of tetradecane filling in a $180 \mu\text{m}$ by $400 \mu\text{m}$ rectangular groove is plotted in Figure 5(b). The height of fluid in rectangular groove varies from 0 to $400 \mu\text{m}$ by step of $10 \mu\text{m}$. The black scatterplot of spoof SPPs sensing is simulated by COMSOL software and red line represents the fit curve.

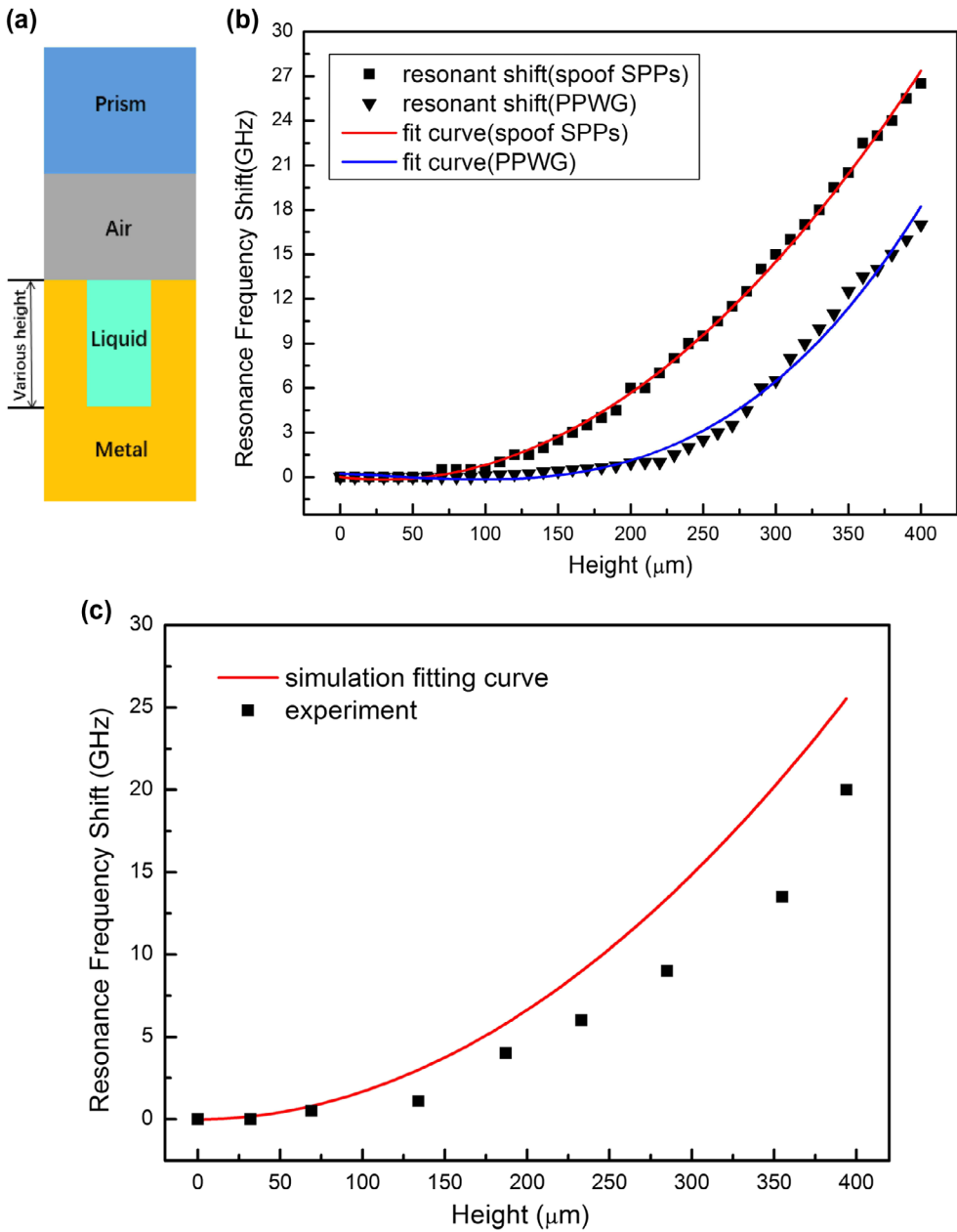


Figure 5. (a) A unit cell of the fluid fill height sensor. (b) The plot of simulated shift in resonance frequency vs. height of tetradecane filling in 180 μm by 400 μm rectangular grooves. (c) Plots of observed shift in resonant frequency for spoof SPPs, obtained experimentally, and simulated.

Meanwhile, the plot of the relation between resonant shift and fluid height based on PPWG [19] is also exhibited in Figure 5(b).

As can be seen from the Figure 5(b), the sensitivity of fluid fill height sensor based on spoof SPPs is much higher than that on the PPWG platform [19]. First of all, no matter with

spoof SPPs or PPWG, the measurable resonant shift is required with a minimum filling height. The value of minimum height is 70 and 100 μm for spoof SPPs and PPWG, respectively. In other words, the value of filling height less than 100 μm can't be detected by PPWG while the spoof SPPs can meet this requirement. Secondly, from the whole point of view, the spoof SPPs is more sensitive to the change of fluid fill height. From 100 to 400 μm , the resonant shift of PPWG changes by 17 GHz, while the spoof SPPs measures a change of 26.5 GHz. Thirdly, the value of resonant shift of spoof SPPs is much higher than the value of PPWG at the same height. For example, resonant shift of spoof SPPs at the height of 250 μm is 9.5 GHz, while the shift of PPWG at the same height is only 2.5 GHz. The physical reason is as follows. The spoof SPPs interact with liquid within several grooves. However, in PPWG, the interaction length between THz wave and liquid is only within single groove. That is, the spoof SPPs have a much larger interaction length (several grooves) than the rather limited interaction length (single groove) of PPWG. This factor greatly enhances the sensitivity of the proposed sensor which shows higher sensitivity than the sensitivity of PPWG. In summary, the fluid fill height sensing based on spoof SPPs is much more advantageous than that based on PPWG.

We experimentally measured the performance of fluid height sensor as shown in Figure 5(c), which is in good agreement with simulation. In order to keep the fluid height h_{fluid} in each groove the same, the sample was etched with two extra grooves on metal surface, which intersect with all fluid grooves perpendicularly. The tested fluid flowed through the extra grooves and then flowed into each groove. The groove is a rectangle with period $p = 300 \mu\text{m}$, height $h = 180 \mu\text{m}$ and width $w = 180 \mu\text{m}$. These rectangular grooves were etched in rectangular metal plate with length $l_p = 4 \text{ cm}$ and width $w_p = 2 \text{ cm}$. Therefore, the height in each groove can be calculated roughly by mathematical formula $h_{\text{fluid}} = V_g / (w * w_p * N)$, where $N = \frac{l_p}{p}$ and is the number of grooves and V_g is the volume of fluid in grooves. The experimental dots from left to right in Figure 4 are (0 μm , 0 GHz), (32 μm , 0 GHz), (69 μm , 0.5 GHz), (134 μm , 1.1 GHz), (187 μm , 4 GHz), (233 μm , 6 GHz), (285 μm , 9 GHz), (355 μm , 13.5 GHz) and (394, 20 GHz).

In addition, the refractive index ($n_d = 1.4224$) of tested fluid filled in the groove is higher than the value (1.39) of $n_p \sin(\theta_{\text{int}})$. The physical reason for this phenomenon is that the sensing structure plotted in Figure 6(a) is quite different from the conventional Otto model plotted in Figure 6(d). Here we plotted the dispersions of both structures, as shown in Figure 6(b) and (e). From dispersion spectrum, we can see that there are 10 intersections in Figure 6(b) but 3 intersections in Figure 6(e), which correspond to 4-layer structure and 3-layer structure, respectively. We note that coupling of the spoof SPPs occurs when $n_p \sin(\theta_{\text{int}})$ is equal to k_{sspp} / k_0 , so each intersection indicates the certain resonance frequency in different fluids. In Figure 6(a), the fluid is just filled in rectangular groove and the gap above groove is filled with air. This means that the evanescent wave deviated from total reflection will always breakthrough the air and liquid layers and excited spoof SPPs in structured surface. However, prism is in direct contact with tested fluid in three-layer structure. Therefore, the condition of total reflection will be destroyed when the refractive index of fluid is higher than prism, then coupling of the spoof SPPs do not occur. So, the refractive index of liquid in three-layer structure should be lower than prism. Such difference means that fluid with refractive index higher than prism is suitable for fluid height sensor in four-layer structure compared to fluid with limited refractive index in three-layer structure.

In order to verify the effectiveness of this method, a group of reflectivity spectrums for 10 fluids filled in 2 different structures was plotted in Figure 6(c) and (f), respectively.

Ten fluids with refractive index from 1.0 to 2.0 were simulated to obtain reflectivity spectrums in Figure 6(c) and (f) using the structure exhibited in Figure 6(a) and (d), respectively. The Figure 6(c) clearly indicates that spoof SPPs coupling still occurs even though refractive

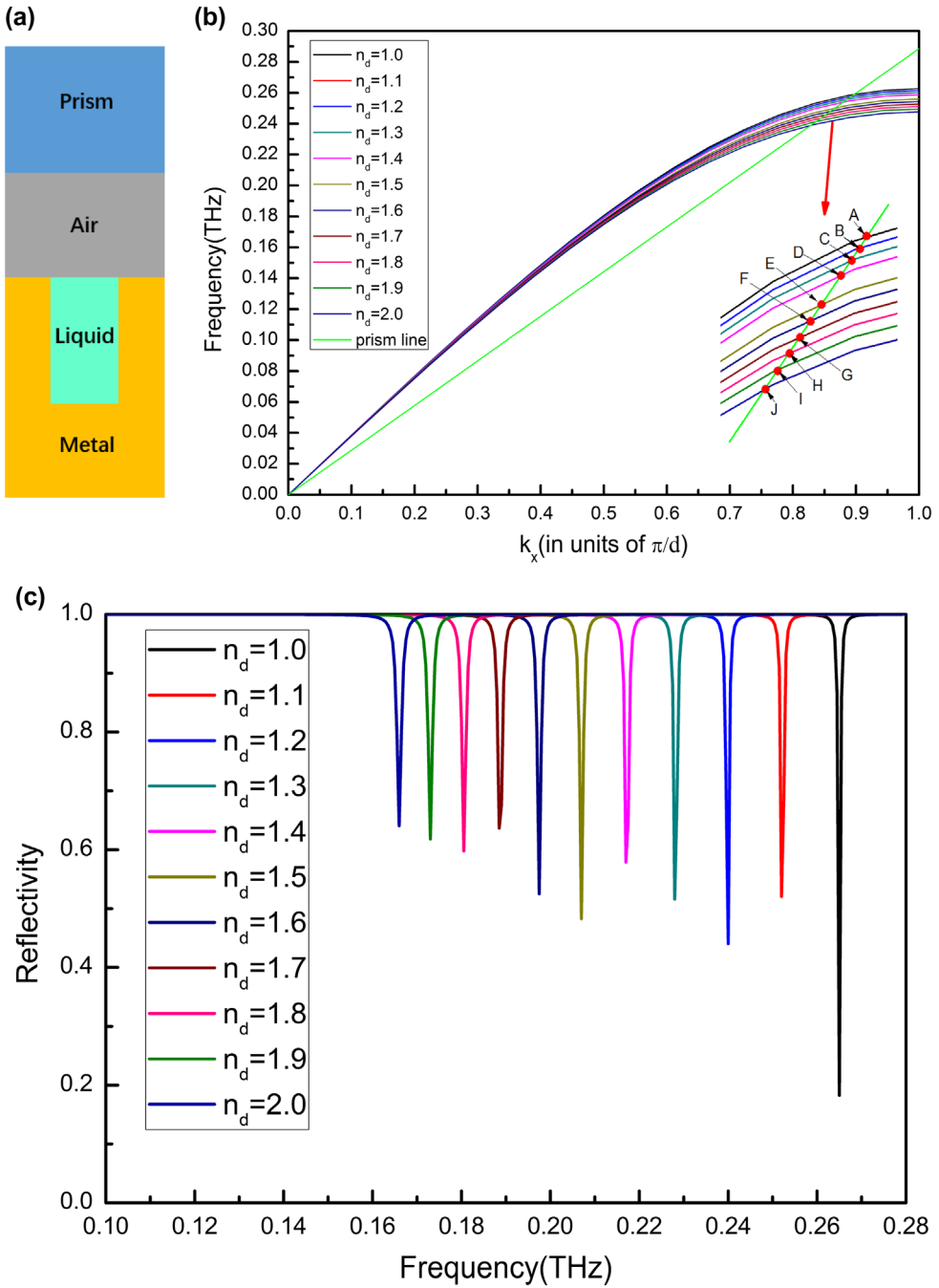


Figure 6. The unit cell of four-layer (a) and three-layer (d) structure. A group of dispersion and reflectivity spectrums for 10 fluids with different refractive index in 4-layer (b) (c) and 3-layer (e) (f) structure.

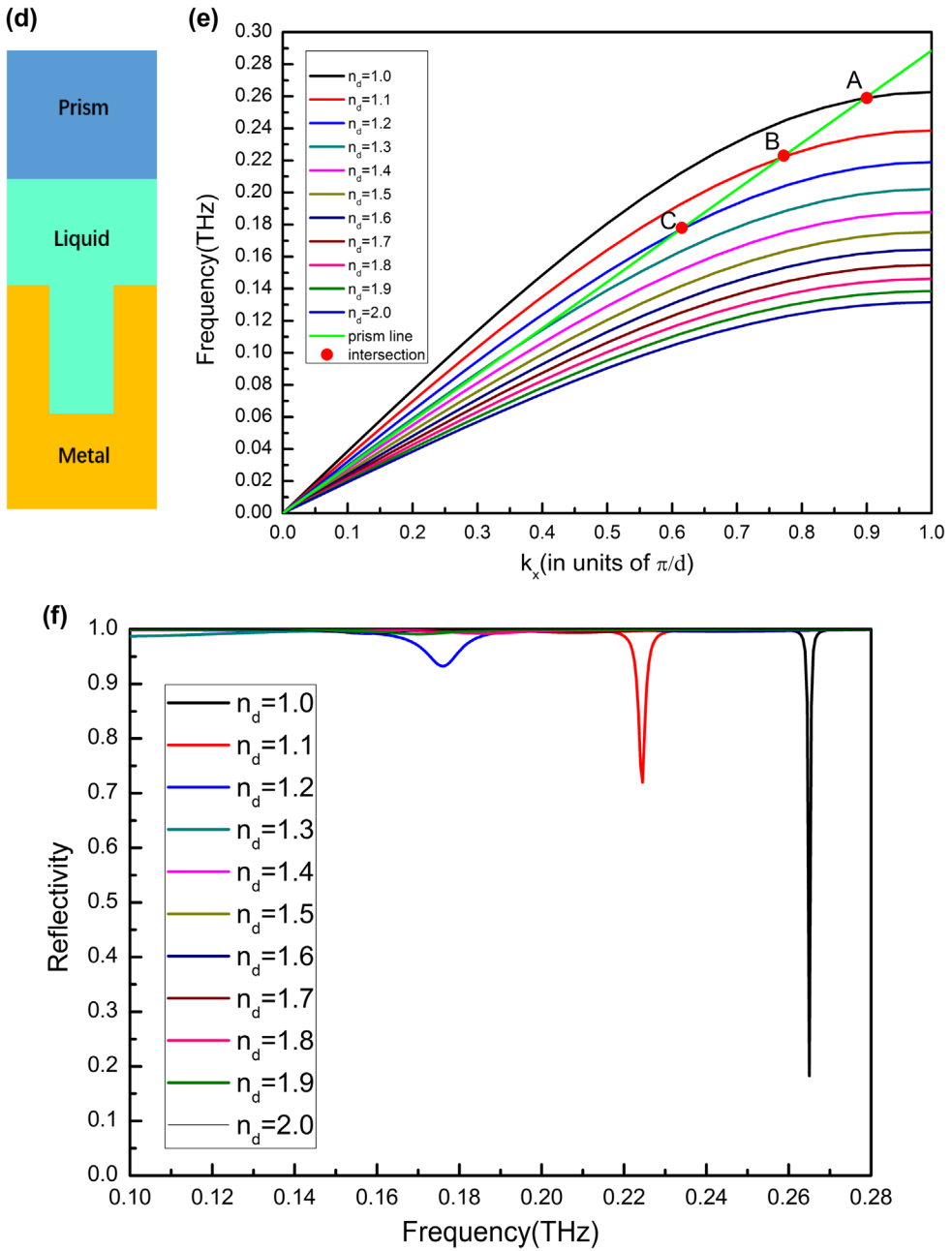


Figure 6. (Continued).

index of fluid is equal to 2.0. Note that the reflectivity spectrum is narrow for each of fluids. The narrow spectrum represents a high Q -factor. For example, the full width at half maximum (FWHM) Δf_{sp} is 1.2 GHz and the Q -factor is up to 134 when $n_d = 2.0$, which guarantees high sensitivity. However, there are only three dips in Figure 6(f), which is corresponding to three intersections in Figure 6(e).

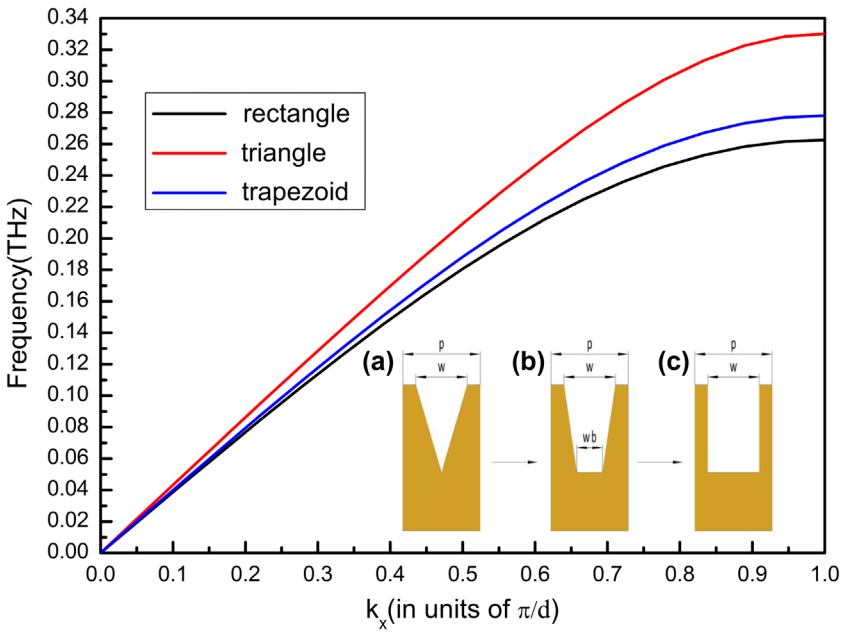


Figure 7. The dispersion curves of SSPPs supported by triangle, trapezoid and rectangle groove. The insets represent the triangle (a), trapezoid (b), and rectangle (c) geometry, respectively.

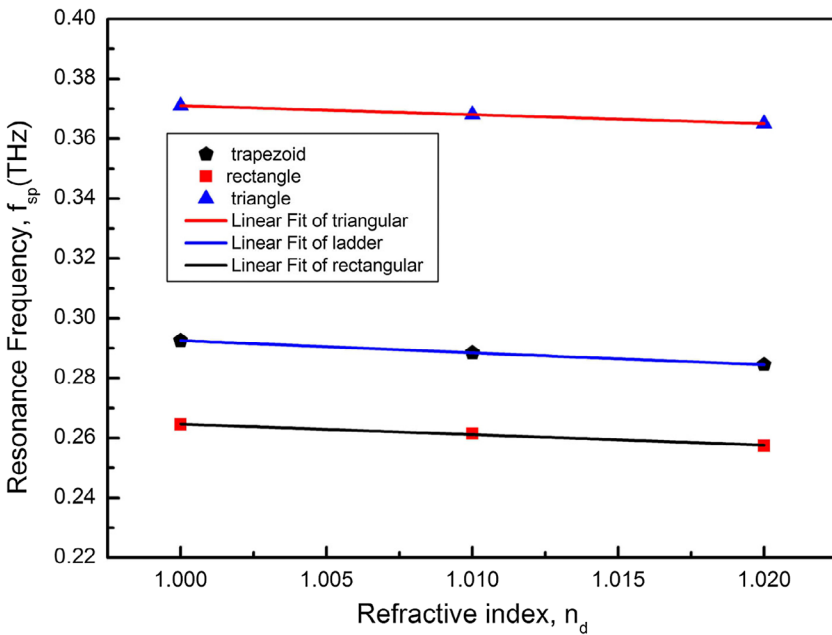


Figure 8. The comparison of sensitivity of spoof SPR sensors supported by triangle, trapezoid, and rectangle geometries. The red, green, and black solid lines are linear fits of resonant frequency corresponding to the sensitivity of 0.3, 0.4 and 0.35 THz/RIU, respectively.

After realizing the spoof SPR sensing system supported by 1D rectangular groove, a further study shows that the shape of groove will affect sensitivity. Here, we take rectangle, triangle and trapezoid as an example. The parameters of the groove are that $p = 300 \mu\text{m}$ and $h = 180 \mu\text{m}$. The trapezoid will turn into triangle eventually when the length of the bottom is zero. The transformation is shown as inset in Figure 7. The rectangle, trapezoid, and triangle structures represent the bottom $w_b = 180 \mu\text{m}$, $120 \mu\text{m}$ and $0 \mu\text{m}$, respectively. Figure 8 plots the calculated dispersion relations of these three structures. It is clear that the asymptotic frequency of dispersion curve increases with the decrease of bottom.

Figure 8 presents a direct comparison of the sensitivity of spoof SPR sensor supported by these three geometries. Just like the rectangle groove mentioned before, the relationship of resonant frequency and refractive index is still nearly linear with the cases of triangle and trapezoid groove. The red, blue, and black solid lines are linear fittings given by $f_{\text{sp}} = -0.3n_d + 0.671$, $f_{\text{sp}} = -0.4n_d + 0.693$ and $f_{\text{sp}} = -0.35n_d + 0.615$, which offer sensitivities of 0.3, 0.4 and 0.35 THz/RIU for triangle, trapezoid, and rectangle groove, respectively. Obviously, the sensitivity of the trapezoid groove is the highest, which makes the spoof SPPs very promising for sensing tiny change of refractive index.

5. Conclusions

In conclusion, we have investigated the performance of fluid fill height sensing supported by spoof SPPs. First we proved the existence of spoof SPPs on metal etched with rectangular grooves and discussed it in detail. After excitation of spoof SPPs, we designed a fluid fill height sensor which is much more sensitive than PPWG [19]. On the basis of fluid fill height sensing technology, we provided a four-layer structure to substitute for conventional three-layer Otto model in order to detect high refractive index fluid. We hope this technology can benefit the THz spoof SPPs sensing.

Disclosure statement

No potential conflict of interest was reported by the authors.

Funding

This work was supported in part by the National Program on Key Basic Research Project of China (973 Program) [grant number 2014CB339806]; the Major National Development Project of Scientific Instrument and Equipment [grant number 2017YFF0106300], [grant number 2016YFF0100503]; National Natural Science Foundation of China [grant number 61671302], [grant number 61722111]; Program of Shanghai Pujiang Program [grant number 17PJD028]; the Key Scientific and Technological Project of Science and Technology Commission of Shanghai Municipality [grant number 15DZ0500102]; Shanghai leading talent [grant number 2016-019]; and Young Yangtse Rive Scholar [grant number Q2016212].

ORCID

Lin Chen  <http://orcid.org/0000-0002-6848-5257>

References

- [1] Sihvola A, Qi J, Lindell IV. Bridging the gap between plasmonics and zenneck waves. *IEEE Antennas Propag.* 2010;52(1):124–136.

- [2] Huang CP, Zhu YY. Plasmonics: manipulating light at the subwavelength scale. *Acta Passiva Electron Compon*. 2007;2007(2007):9–13.
- [3] Pitarke JM, Silkin VM, Chulkov EV, et al. Theory of surface plasmons and surface-plasmon polaritons. *Rep Prog Phys*. 2006;70(1):1–24.
- [4] Homola J, Yee SS, Gauglitz G. Surface plasmon resonance sensors: review. *Sens Actuators, B*. 1999;54(1–2):3–15.
- [5] Pattnaik P. Surface plasmon resonance. *Appl Biochem Biotechnol*. 2005;126:79–92.
- [6] Pendry JB, Martín-Moreno L, García-Vidal FJ. Mimicking surface plasmons with structured surfaces. *Science*. 2004;305(5685):847–848.
- [7] García-Vidal F, Martín-Moreno L, Pendry, JB. Surfaces with holes in them: new plasmonic metamaterials. *J Opt A: Pure Appl Opt*. 2005;7(2):S97–S101.
- [8] Rusina A, Durach M, Stockman MI. Theory of spoof plasmons in real metals. *Appl Phys A*. 2010;100(2):375–378.
- [9] Chen L, Zhu Y, Zang X, et al. Mode splitting transmission effect of surface wave excitation through a metal hole array. *Light Sci Appl*. 2013;2(3):e60.
- [10] Gric T. Spoof plasmons in corrugated transparent conducting oxides. *J Electromagn Waves Appl*. 2016;30(6):721–727.
- [11] Gric T, Wartak MS, Cada M, et al. Spoof plasmons in corrugated semiconductors. *J Electromagn Waves Appl*. 2015;29(14):1899–1907.
- [12] Chen L, Wei Y, Zang X, et al. Excitation of dark multipolar plasmonic resonances at terahertz frequencies. *Sci Rep*. 2016;6:22027.
- [13] Chen L, Xu N, Singh L, et al. Defect-induced fano resonances in corrugated plasmonic metamaterials. *Adv Opt Mater*. 2017;5(8):1600960.
- [14] Ng B, Wu J, Hanham SM, et al. Spoof plasmon surfaces: a novel platform for THz sensing. *Adv Opt Mater*. 2013;1(8):543–548.
- [15] Yao H, Zhong S. High-mode spoof SPP of periodic metal grooves for ultra-sensitive terahertz sensing. *Opt Express*. 2014;22(21):1–12.
- [16] Zhang Y, Hong Z, Han Z. Spoof plasmon resonance with 1D periodic grooves for terahertz refractive index sensing. *Opt Commun*. 2015;340:102–106.
- [17] Xu Z, Mazumder P. Bio-sensing by Mach-Zehnder interferometer comprising doubly-corrugated spoofed surface plasmon polariton (DC-SSPP) waveguide. *IEEE Trans Terahertz Sci Technol*. 2012;2(4):460–466.
- [18] Chen X, Fan W. Ultrasensitive terahertz metamaterial sensor based on spoof surface plasmon. *Sci Rep*. 2017;7(1):2092.
- [19] Astley V, Reichel KS, Jones J, et al. A mode-matching analysis of dielectric-filled resonant cavities coupled to terahertz parallel-plate waveguides. *Opt Express*. 2012;20(19):21766–21772.
- [20] Chen L, Xu J, Gao C, et al. Manipulating terahertz electromagnetic induced transparency through parallel plate waveguide cavities. *Appl Phys Lett*. 2013;103(25):251105.
- [21] Chen L, Gao C, Xu J, et al. Observation of electromagnetically induced transparency-like transmission in terahertz asymmetric waveguide-cavities systems. *Opt Lett*. 2013;38(9):1379–1381.
- [22] Chen L, Cheng Z, Xu J, et al. Controllable multiband terahertz notch filter based on a parallel plate waveguide with a single deep groove. *Opt Lett*. 2014;39(15):4541–4544.
- [23] Chen L, Cao Z, Ou F, et al. Observation of large positive and negative lateral shifts of a reflected beam from symmetrical metal-cladding waveguides. *Opt Lett*. 2007;32:1432–1434.
- [24] Ordal MA, Long LL, Bell RJ, et al. Optical properties of the metals Al, Co, Cu, Au, Fe, Pb, Ni, Pd, Pt, Ag, Ti, and W in the infrared and far infrared. *Appl Opt*. 1983;22(7):1099–1119.
- [25] Seitz F, Turnbull D. *Solid state physics*. New York (NY): Academic Press; 1958.
- [26] Cheng Z, Chen L, Zang X, et al. Ultrathin dual-mode filtering characteristics of terahertz metamaterials with electrically unconnected and connected U-shaped resonators array. *Opt Commun*. 2015;342:20–25.
- [27] Cheng Z, Chen L, Zang X, et al. Tunable plasmon-induced transparency effect based on self-asymmetric H-shaped resonators meta-atoms. *J Opt*. 2015;17(3):035103.
- [28] Chen L, Truong KV, Cheng Z, et al. Characterization of photonic bands in metal photonic crystal slabs. *Opt Commun*. 2014;333:232–236.
- [29] Hirori H, Nagai M, Tanaka K. Destructive interference effect on surface plasmon resonance in terahertz attenuated total reflection. *Opt Express*. 2005;13(26):10801–10814.
- [30] Laib JP, Mittleman DM. Temperature-dependent terahertz spectroscopy of liquid n-alkanes. *J Infrared, Millimeter, Terahertz Waves*. 2010;31(9):1015–1021.